Irrigation water demand sensitivity to climate variability across the Contiguous United States

Wanshu Nie[1,2], Benjamin F. Zaitchik[1], Matthew Rodell[3], Sujay V. Kumar[3], Kristi R. Arsenault[3,4], Hamada S. Badr[1]

[1]Department of Earth and Planetary Sciences, Johns Hopkins University, Baltimore, Maryland

[2]NASA GESTAR, Greenbelt, Maryland

[3]Hydrological Science Laboratory, NASA Goddard Space Flight Center, Greenbelt, Maryland

[4]Science Applications International Corporation, McLean, Virginia

Corresponding author: Wanshu Nie (nwanshu1@jhu.edu)

Key Points:

- Widespread sensitivity of irrigation water use to precipitation is found in both model and available reports.
- Temperature and interactions of temperature – precipitation sensitivity vary by region and season and might be underestimated by the model.
- Geographical disconnects exist between aquifers that are stressed by pumping and the basins that exhibit strong climate sensitivities.

Abstract

Climate variability is an important driver of irrigation water use in many regions. Efforts to anticipate climate change impacts on future water availability can benefit from understanding how irrigation water demand has responded to these drivers to date. Here we apply satellite-derived data, meteorological reanalysis, an advanced land surface model, and available state-level reports to quantify irrigation demand sensitivities to temperature and precipitation across the Contiguous United States, for the period of 2002-2017. As expected, strong negative correlations are found between precipitation and irrigation withdrawals, both simulated and reported. Temperature sensitivities, however, vary by region and season, as do the interactive effects of temperature and precipitation on irrigation. Climate-induced irrigation variability is largest in transitional climate zones. These transitional zones are generally separate from the regions where rates of irrigation withdrawals are greatest, such that climate-induced variability in irrigation demand represents a water resource consideration that is distinct from chronic over-pumping.

1. Introduction

In the United States, irrigation accounts for ~40% of total freshwater withdrawal and more than 60% of total freshwater consumption [*Dieter*, 2018]. Approximately 60% of irrigated areas are supplied by groundwater resources [Siebert et al., 2010; Scanlon et al., 2012]. In recent decades, there has been dramatic groundwater depletion in the southern High Plains and California Central Valley, as observed by both ground-based measurements and Gravity Recovery and Climate Experiment (GRACE) satellite data [Russo and Lall, 2017; Rodell et al., 2018]. In these regions, intensive abstraction at the rates currently practiced cannot be balanced by groundwater recharge and could be further intensified under droughts due to surface water shrinkage [*Zou et al.*, 2018]. Over-pumping of groundwater also induces secondary effects, such as land subsidence due to compaction in the subsurface aquifer system [*Liu et al.*, 2019] and aquifer contamination [*Jasechko et al.*, 2017]. Even in more humid regions, water withdrawals for irrigation have impacts on surface water availability and water quality [*Baker et al.*, 2012].

Irrigation applications, and associated groundwater extractions, are inextricably linked to climate variability. Irrigation demand is affected by precipitation, temperature, and other meteorological variables, such that total pumping for irrigation can vary as a function of climate conditions in many regions—climate-induced pumping [Russo and Lall, 2017]. While a scarcity of fresh water resources has already emerged in many parts of the world under current climate conditions, climate change may pose an additional threat to water security should warming and/or a shift in precipitation patterns ever lead to changes in water supply [Schewe et al., 2014]. Climate-induced pumping might exacerbate these water shortages. Additionally, the tendency of an irrigated region to increase water use in response to precipitation shortage or elevated temperatures is an indicator of the sensitivity of that region's irrigated agriculture to climate variability. Therefore, understanding the impact that climate variability has on irrigation water use is important when assessing the vulnerability of irrigation developments from a perspective of water resource depletion and of changes in water demand. This could be particularly relevant in the context of climate change, as recent work indicates that warming is expected to reduce groundwater storage in natural systems that are not already water-limited on account of increased evapotranspiration [Condon et al., 2020].However, spatially and temporally distributed

observations of irrigation water extraction and consumption are limited, constraining the assessment of irrigation responses.

One way to overcome this data gap is to simulate irrigation water use through global hydrological models (GHMs) or land surface models (LSMs) implemented with reasonable irrigation parameterizations and assumptions. Modeling efforts have been undertaken to improve the representation of human water use in these models [*Nazemi and Wheater*, 2015; *Pokhrel et al.*, 2016; *McDermid et al.*, 2017; *Wada et al.*, 2017; *Felfelani et al.*, 2018; *Scanlon et al.*, 2018; *de Graaf et al.*, 2019; *Devanand et al.*, 2019; *Yin et al.*, 2020; *Condon et al.*, 2019]. Nonetheless, limitations exist in current studies, including, in different cases: 1) ignoring where the withdrawals occur [*Evans and Zaitchik*, 2008; *Leng et al.*, 2013; *Yilmaz et al.*, 2014; *Lawston et al.*, 2015]; 2) ignoring interannual changes in irrigation land use or in source water partitioning [*Wada et al.*, 2010; *Leng et al.*, 2014; *Pokhrel et al.*, 2015]; 3) ignoring the interactions between soil moisture and groundwater [*Van Beek et al.*, 2011; *Wada et al.*, 2014]; 4) irrigating based on a climatologically fixed growing season that does not account for management responses to extreme events such as drought [*Lawston et al.*, 2017]; and 5) calibrating models using non-physical parameters that may not provide skill in future water use projections [*Döll et al.*, 2012; *Eicker et al.*, 2014].

We have modified an advanced land surface model to include a demand-driven irrigation scheme and source water accounting [Nie et al., 2018]. Here, we perform simulations with this modeling system that make use of multiple time-varying data sources (irrigation fraction, groundwater irrigation percentage, and greenness vegetation fraction) to estimate the timing, location, and seasonal to interannual variability of conditions relevant to irrigation water use: 1) irrigation fraction datasets updated every 5 years obtained from the Moderate Resolution Imaging Spectroradiometer (MODIS) Irrigated Agriculture Dataset for the United States (MIrAD-US) that provide the location and fraction of the irrigated area within a model grid cell; 2) USGS-based groundwater irrigation percentage datasets updated every 5 years that allocate surface water and groundwater sources to irrigation demand; and 3) MODIS-Normalized Difference Vegetation Index (NDVI) based time-varying monthly greenness vegetation fraction (GVF) that represents the coverage of vegetation and is used to estimate the timing of growing seasons and the status of root depth. Using retrospective model simulations, we quantify the impacts that precipitation and temperature variability have on simulated irrigation quantity. Results are analyzed by region, growing season, and irrigation water source to understand patterns of climate sensitivity, as simulated by the model. Finally, we compare the climate sensitivity of our demand-driven irrigation simulation to climate sensitivity inferred from available state-level reports on irrigation water use.

2. Data and Methods

2.1 The irrigation scheme and inputs

In this study, simulation was performed using the Noah-Multiparameterization Land Surface Model [Noah-MP LSM; *Niu et al.*, 2011], version 3.6, within the framework of NASA's Land Information System [LIS; *Kumar et al.*, 2006]. Noah-MP contains a multilayer snowpack, four soil layers with a total soil depth of two meters and a simple groundwater scheme allowing for soil moisture-groundwater interaction and related runoff production. Surface energy fluxes are computed using resistor network theory while water movement in the soil layers is simulated

using the Richards equation. For groundwater, the temporal variation of the storage is determined by the residual of recharge rate minus discharge rate. The recharge rate is parameterized following Darcy's law, whereas the discharge rate (base flow or subsurface runoff), along with the surface runoff are parameterized by a TOPMODEL-based scheme as exponential functions of the water table depth [*Niu et al.*, 2007]. The water table depth is converted from the aquifer water storage scaled by the specific yield, which is set to be a global constant of 0.2 for Noah-MP. Building on the Noah LSM [*Ek et al.*, 2003], Noah-MP advances its structure by better accounting for canopy energy balance, vegetation phenology, groundwater and snow dynamics [*Yang et al.*, 2011], and allowing for a combination of multi-physics options such as radiative transfer and runoff schemes. A detailed description of the model and its performance can be found in Niu et al. [2011] and Yang et al. [2011].

In previous work [*Nie et al.*, 2018], we introduced a demand-driven sprinkler irrigation scheme to Noah-MP, in which the three key rules to trigger the irrigation in this modeling framework include the irrigation location (where to irrigate), the timing (when to irrigate) and the amount (how much to irrigate). The percent irrigated area is obtained from the MODIS Irrigated Agriculture Dataset [MIrAD-US; *Brown and Pervez*, 2014]available for 2002, 2007, and 2012 at 250 m spatial resolution, providing the location and fraction of the irrigated area within a model grid cell. Since MIrAD-US is only updated once every five years, we use a single dataset for five years, until the next dataset becomes available; i.e., dataset of 2002 is used for 2002-2006, 2007 is used for 2007-2011, and finally, 2012 for 2012-2017. The time-varying GVF, derived from monthly MODIS NDVI composites and MODIS-IGBP land cover data set at 0.05° spatial resolution [*Nie et al.*, 2018], is used to define the timing of irrigation, which begins and ends when a certain threshold within the long-term range GVF at the grid cell is exceeded. Then the scheme checks if the current root zone soil moisture availability falls below a certain threshold for each morning at 0600 LT local time, which is set to 52% of the plant-available soil water storage. The root zone depth is the product of the time-varying GVF and the maximum depth of the root zone [*Ozdogan et al.*, 2010]. Once irrigation is triggered, the irrigation water amount is calculated as the volume required to bring the root zone soil moisture deficit up to field capacity and it is applied at every time step between 0600 to 1000 local time at a constant rate. Both the maximum root depth and field capacity are drawn from static tables as a function of crop types and soil types, respectively. This approach to simulating sprinkler irrigation in Noah-MP builds upon the work of Ozdogan et al. [2010].

For our water source partitioning scheme, we assume that irrigation water is sourced from some combination of groundwater and surface water. The ratio of groundwater to total irrigation water is derived from county-level data included in the USGS water use report (https://water.usgs.gov/watuse/data/), which are available at 5-year intervals for 2000-2015. The scheme then subtracts the groundwater irrigation amount from the model's groundwater aquifer storage term, and the water table depth and groundwater storage are updated accordingly. We do not attempt to represent the full complexity of irrigation practices across the Contiguous United States (CONUS) in our model. Instead, in order to obtain results that can be cleanly interpreted in terms of climate sensitivity of irrigation demand, we make the following simplifying assumptions: 1) all irrigation is simulated as sprinkler irrigation for row crops; 2) water use efficiency is not considered, as we want to avoid introducing additional uncertainties to the system; 3) crop management and deficit irrigation are not directly accounted for due to limited data sources and coverage. Notwithstanding these simplifications, incorporating time-varying irrigation fractions, groundwater ratios and GVF into our simulation at their greatest available

frequency allows the model to capture some management effects, including interannual variability and trends in irrigation water use in response to short-term climate variability.

The simulation is performed over CONUS at 0.125° spatial resolution at a 15 min computational time step for the period 2002-2017 after a 78-yr spin-up (twice over the period of 1980-2018). Noah-MP is applied in offline mode (not coupled to an atmospheric model), and is driven by National Land Data Assimilation System-Phase 2 [NLDAS-2; *Xia et al.*, 2012] meteorological fields, including 2-m air temperature, 2-m specific humidity, 10-m wind speed, surface pressure, precipitation, incoming shortwave and longwave radiation. The model is configured using the MODIS-IGBP land cover at 1 km, State Soil Geographic [*Schwarz and Alexander*, 1995] soil texture at 1 km and the Shuttle Radar Topography Mission elevation at 30 m [*Farr et al.*, 2007]. As we choose to prescribe the vegetation conditions using time-varying GVF, the model does not use the dynamic vegetations scheme within Noah-MP. Model output fields include states such as soil moisture, groundwater and surface fluxes such as latent, sensible and ground heat flux, and runoff.

2.2 Assessing climate sensitivity

To evaluate the realism of simulated irrigation water use, we compared the model's annual irrigation totals with the USGS reported irrigation amount at state level. These estimates are available for 2005, 2010, and 2015. Note that the USGS reported water use for 2005 and 2010 does not distinguish between consumptive and non-consumptive water uses while the report for 2015 includes both total and consumptive water use estimation, which offers a useful point of comparison for our simulated irrigation water use. While our model includes some non-consumptive use—i.e., water returned via recharge to groundwater or as surface runoff— in addition to consumptive use, it does not include conveyance losses or other off-field losses and on-field application inefficiencies, part of which can account for a significant amount of non-consumptive water use in real irrigation settings. The USGS consumptive use estimate in 2015, therefore, provides a useful lower bracket on water use, and we might expect our simulated irrigation demand to fall near that lower bracket. To evaluate irrigation impact on water fluxes, we compare the simulated terrestrial water storage anomalies with the GRACE-derived observations. The full record of Level 3, Version RL05, monthly gridded mascon GRACE data at $0.5° \times 0.5°$ resolution derived by National Aeronautics and Space Administration Jet Propulsion Laboratory (JPL) [*Wiese et al.*, 2016] is used in this study.

To explore the relationship between irrigation water use and short-term climate variability, we examine temporal correlations between growing season meteorological variables—seasonal precipitation (P) and 2-m air temperature (T) from NLDAS-2 —and simulated irrigation water use for all actively irrigated grid cells. Rather than using a fixed growing season period or referring to a crop calendar, we define an "effective growing season" for each grid cell. This is done by first locating the peaks in the climatologically-averaged annual cycle of monthly GVF for each grid cell, and then defining the peak month, together with one month before and after it, as an effective growing season. The peaks are detected if they are greater than a defined threshold and can survive Gaussian blurring up to scale 1. Nine major growing season types (GST) are categorized for analysis in which four are defined as the single season type (spring, summer, autumn, winter) while the remaining five are defined as the dual season type (e.g., "spring and autumn"). The spatial patterns of the GSTs for actively irrigated areas are shown in Figure S1.

We then average P, T and simulated irrigation water use in actively irrigated grids within each river basin for each GST (sub-basin hereinafter) and apply a simple multivariate linear regression model: growing season irrigation water use is the response variable, and P, T and their interaction (P*T) are the three predictor variables. We choose this simple statistical approach because we are attempting to understand general relationships rather than to optimize prediction skill. Nine major irrigated river basins are included in the analysis (Figure 1). A GST is included in the analyses for a river basin if the GST represents more than 10% of the basin area. This criterion led to identification of 16 basin-by-GST combinations. They include three single season GSTs (spring, summer and autumn) and one dual season GST (spring-autumn). The annual time series averaged over each sub-basin are normalized by subtracting the mean and dividing by standard deviation so that the regression coefficients are comparable to each other. Note that for the interaction term, we standardize P and T before multiplying them in order to reduce the structural multicollinearity caused by strong correlation between P and its interaction with T. As short-term climate influence on irrigation demand may largely vary by basin, the inclusion of these three terms for the regression model may be overfitted for some basins. To test on the influence of overfitting, we reconduct the regression for each basin by correspondingly removing the predictor variables with insignificant coefficients informed by the full model, which we then refer to as the "reduced model". In addition to basin scale analysis, we also apply the linear regression at the grid cell scale for actively irrigated area. For both cases, a Shapiro-Wilk test is performed to check the normality of the residuals for the linear regression models and more than 90% of the actively irrigated area meets the assumption of residual normality. Basins or grid cells that failed to pass the test have been removed from the analyses.

2.3 Observation datasets

Annual irrigation water use reports are obtained for Kansas, Texas, California and Mississippi in order to evaluate the modelled climate sensitivities. These four states are chosen because they are the only databases that we found that are publicly available. The states also happen to be among the most intensively irrigated and the most agriculturally productive states over CONUS. Statewide calendar year annual averages from 2002 to 2017 for Kansas and Texas are provided by the Kansas Department of Agriculture, Division of Water Resources (per request) and the Texas Water Development Board (http://www.twdb.texas.gov/) based on the data submitted by the irrigation water right owners. Growing season irrigation amount for row crops from 2003-2011 for Mississippi are obtained from Massey et al. [2017], who generated the estimates by applying the power conversion coefficient method to the electrical power consumption records of the irrigation pumping wells. Unlike the cases in Kansas and Texas, private groundwater pumping for irrigation is rarely metered in California [Valley, 2009], therefore, the annual water year estimates from 2002-2015 produced by the California Simulation of Evapotranspiration of Applied Water (Cal-SIMETAW) model are used as a proxy for observations. The model estimates irrigation water demand based on an evapotranspiration demand approach, the aim of which is to improve the accuracy of water use estimates for the California Water Plan [Orang et al., 2013]. The correlation and regression analyses are performed for both reported estimates and the corresponding simulated irrigation water use for these four states based on both the annual averages and the effective growing seasons.

3. Results

3.1 Irrigation water use

The largest irrigated areas in CONUS are located in the Lower Mississippi Region (LMR), the High Plains Aquifer crossing the Missouri Region (MR) and the Arkansas-White-Red Region (AWRR), the California Region (CR), the Pacific Northwest Region (PNR) along the Snake River. There is also actively irrigated land with smaller extent in the eastern CONUS, including the Great Lakes Region (GLR), Upper Mississippi Region (UMR) and South Atlantic-Gulf region (SAGR) (Fig. 1 (a)). According to USGS, in 2000, more than 50% of irrigation water use was from groundwater for all basins except the CR and the PNR, which were dominated by surface water irrigation (Figure 1 (b)). Within the short period of 2000-2015, the coverage and locations of irrigation areas and the partitioning of irrigation water sources changed substantially, according to the MIrAD-US irrigation fraction and USGS-based groundwater irrigation percentage datasets. As shown in Figure 2, irrigation fraction increased about 4% for the LMR in 2012 compared to 2002, while the percentage contribution of groundwater decreased by 4.5%. In the CR, in contrast, the irrigation fraction dropped by about 2%, while groundwater contribution to irrigation increased over time by 26%. The dramatic shift towards groundwater for the CR is likely due to the long-lasting drought that affected the region during this period; the use of groundwater to prevent crop water stress during this drought led to serious groundwater depletion issues and threatened groundwater sustainability [Scanlon et al., 2012]. Modeling studies [Pokhrel et al., 2012; Leng et al., 2014; Lawston et al., 2015] often use a static map to represent irrigated area or ignore the source of water that is applied in irrigation, which has limited their ability to study long-term irrigation water use variability and its impact on both surface water and groundwater. While the irrigation scheme used in this study is demand-driven, by incorporating time-varying irrigation fraction and groundwater irrigation percentage maps into our model, we are able to indirectly simulate irrigation water use associated with land use change, irrigation expansion, and water management.

Figure 3 (a) compares simulated and USGS reported irrigation water use from groundwater and surface water for the top 10 irrigated states for the years 2005, 2010, and 2015, with the remaining states shown in Figure S2. In general, our simulated annual irrigation water use is consistent with the USGS reports in terms of states and years, though the simulated quantities are mostly lower than the USGS estimates. The underestimation of simulated irrigation water use compared to USGS reports is likely due to the assumption inherent to the model that irrigation practices are logical and efficient, whereas in the real world there are off-field losses and other inefficiencies that increase total water usage.

As of 2015, the USGS report began to provide consumptive irrigation water use estimates that are a better reference for comparison (Figure 3 (b)), as the simulated irrigation amounts are mostly consumptive, with only a small proportion returning to water bodies as either surface runoff or groundwater recharge. For example, our simulated total water use for California in 2015 was 16.1 km3, which is only 61% of the USGS reported total water use, but is much closer to the USGS reported consumptive water use of 20.3 km^3. The model tends to underestimate the consumptive water use over western CONUS while overestimating over central CONUS. For eastern regions, the irrigation amount is relatively small so that the uncertainty is much larger and more mixed (Figure S3). Overall, the simulated water use regressed on the reported consumptive use has a slope of 0.79, indicating that on average the model underestimates by about 20% relative to consumptive use reports. We consider this to be a reasonable level of agreement considering the uncertainties in the irrigation parameters, modeling methodology,

measurement errors and limited resolution and precision of USGS estimates. Furthermore, our previous studies [Nie et al., 2018; 2019] showed that for the groundwater-fed irrigation dominated High Plains Aquifer including the irrigation scheme improves model agreement with satellite-derived evapotranspiration and soil moisture estimates, GRACE-derived terrestrial water storage (TWS) patterns, and depth-to-groundwater measurements in Texas and Kansas, especially under drought conditions. These results suggest that the model, together with its multiple satellite derived observation inputs, is in general, able to capture the irrigation response to climate variability, extreme conditions, and their impact on water and energy fluxes.

3.2 Relationship to irrigation water source

In general, simulated irrigation demand shows significant sensitivity to same-season precipitation (P) in all growing seasons (Figure 4). At least 73% of the irrigated grid cells have significant negative correlation with precipitation for single season crops, with the highest (90%) for summer crops, while the correlation with temperature (T) is much less significant, with the percentage of irrigation-containing grid cells showing significant sensitivity ranging from 12% for winter crops to 44% for summer crops. Most of the grid cells that have significant correlation with temperature are also significantly correlated with precipitation. However, the percentage showing significant relationships with both P and T is much less for dual season crops than for single season crops, and, more interestingly, the dual season grid cells that are significantly correlated with T are not necessarily significantly correlated with P. The reduced significance effects are mainly attributable to weaker correlations in the second growing season of the calendar year. The strength of the correlations in the earlier season for dual season grid cells is comparable to that of single season grid cells. Overall, simulated short-term climate influences are fairly insensitive to the choice of growing season, so the particular choice of the timing and duration of the effective growing season does not greatly affect the results (Figure S4 and S5).

To investigate connections between irrigation water source and climate-irrigation water use relationships, we further categorize the active irrigated grid cells into three classes: (i) the surface water dominated area, where the groundwater irrigation percentage is lower than 20%; (ii) the groundwater dominated area, where the groundwater irrigation percentage is higher than 80% and (iii) the mixed area, where the groundwater percentage is in between 20% and 80%. As shown in Figure S6, we find that the climate sensitivities of all three water source classes are qualitatively similar. However, uncertainties exist as the groundwater irrigation ratio data are updated every five years, which precludes investigation of transient climate impacts on source water ratios. Nevertheless, previous studies have found that climate variability can have large influence on groundwater storage change through climate-induced pumping, and this effect may be much stronger and faster than the climate's direct effect on groundwater recharge rates [Asoka et al., 2017; Gurdak, 2017; Russo and Lall, 2017]. Recognizing the fast response of groundwater to climate through irrigation withdrawal, assessments of irrigation management must consider both irrigation demand sensitivity to climate variability and the associated aquifer condition as well as groundwater availability.

3.3 Regression analysis

At the basin scale, a linear regression that includes P, T, and a P by T interaction term explains between 33% and 90% of variability in simulated year-to-year irrigation water use (Table 1). For some growing seasons and basins, such as summer crops in the TGR, the AWRR

and the MR, more than 70% of the variance can be captured mainly by the negative relationship between irrigation water use and precipitation. In these situations, the effective growing season coincides with the local rainy season (Figure 5), so it is intuitive that interannual P variability would have a dominant influence on irrigation applications. For other basins, such as summer crops in the CR, the GLR, and spring-autumn crops in PNR, however, temperature provides comparable influence relative to precipitation. It is noteworthy that T is a statistically significant predictor only in the PNR, MR, and GLR basins, which are the three northernmost basins in the study. In the GLR, T is, in fact, the only statistically significant predictor, reflecting the model's sensitivity to evaporative demand in this relatively high rainfall basin. The interaction term is only significant for summer crops in the TGR and autumn crops in the AWRR, both indicating that irrigation water use is more sensitive to the precipitation deficit under higher temperature. The opposite tendency (not statistically significant) is found in the LMR, the CR, the SAGR and spring-autumn crops in the PNR, where warmer conditions weaken the anticorrelated link between precipitation and irrigation water use. The significance and relative contribution of the predictor variables informed by the full model are consistent with those estimated using the reduced model for most basins (Table S1). However, for spring crops in the CR and summer crops in the SAGR, the contribution from P becomes significant after removing T and the interaction term. Moreover, for UMR, both P and T are significantly and contribute comparably to irrigation variability after removing the interaction term.

The CR stands out among the nine river basins, as the regression has particularly poor explanatory power there for both spring crops (41%) and summer crops (33%). The fact that roughly two-thirds of simulated irrigation water use variance is unexplained by P, T and their interaction for the CR is the product of a mixed response of irrigation water use to climate variability. The spatial variation in irrigation response for the CR is shown in the gridded regression analysis (Figure 6), and it shows some evidence that the north-to-south spatial variability of climate over the CR influences diverse sensitivities within the basin, though the pattern is somewhat mixed. For summer crops in California's Central Valley, where the climate condition is extremely dry and there is low in-season precipitation, temperature plays a major role in determining simulated irrigation amount. This result is driven primarily by an observed negative relationship between temperature and GVF—higher temperature estimates from NLDAS-2 are associated with lower MODIS-based GVF values. The lower GVF is a combined product of fallowing and poorer crop growth. The model's irrigation routine responds to this observation of smaller GVF by reducing irrigation applications, as lower (observed) vegetation is an indicator of less irrigation. In the northern CR, irrigation amount is much smaller, as this region receives greater in-season precipitation. Both P and T have comparable contribution to irrigation water variability in this area, but the contribution of T is positive, which is the opposite to that for the Central Valley (Figure 6).

Negative simulated groundwater storage trends are found for all western basins, while there are no significant trends for eastern U.S. basins (i.e. the UMR, the LMR, the GLR and the SAGR), estimated using a Mann-Kendall test to detect monotonic significance at the 5% level and the Theil Sen Slope test for trend magnitude (Table 1). Widespread groundwater declines over irrigated areas are mainly attributed to associated groundwater pumping and drought. Extreme groundwater declines are found in the AWRR for autumn crops, the CR, and the TGR for summer crops, reaching 3.8, 3.0 and 2.3 cm/yr, respectively. The fact that irrigation water use for these basins and seasons is primarily sensitive to precipitation indicates that future warming is less likely to have a direct impact on groundwater sustainability compared to variability of

precipitation. In contrast, regions such as the CR, where there is high climate variability, temperature sensitivity and alarming groundwater depletion, may face greater complexity of direct warming-induced irrigation sensitivities (Figure 6). For basins where the interactions between P and T have relatively larger effects, future warming may influence irrigation water use indirectly, by altering the sensitivity of irrigation demand to precipitation.

We note that the uncertainties in the estimated irrigation demand and in the model physics of deep soil-groundwater interaction can both affect the simulated groundwater response to irrigation water withdrawals. For instance, in our previous studies over the High Plains, the model underestimated groundwater recovery after a severe drought for Nebraska not because of an overestimation of irrigation amount, but largely due to shortcomings in model representation of subsurface hydrology [Nie et al., 2018]. These uncertainties should be considered when interpreting the simulated impact of irrigation on groundwater trends shown in this study. A thorough, observation-based evaluation of groundwater change under irrigation would be highly useful, but is challenging to accomplish at the national scale on account of limited and uneven in-situ groundwater measurement networks. Rather than directly evaluating simulation of groundwater, we compare simulated TWS anomalies with GRACE observations for the top ten irrigated states (Figure S7). The comparison suggests that the model generally captures the irrigation impact on TWS at state scale, with the exceptions of overestimating decline in Nebraska after 2012, as mentioned earlier, and slightly overestimating declines in Texas and Colorado in 2017. We also note that this analysis does not account for carbon dioxide fertilization, which may also influence the water balance in irrigated fields under evolving atmospheric conditions, so our results are best interpreted as an analysis that applies to current and near-future conditions.

It is worth noting that the basins exhibiting greatest climate sensitivity tend not to be in regions that are currently experiencing the greatest water stress (Table 1). Climate-induced irrigation variability is largest in transitional climate zones between humid east and arid west, such as irrigated land within MR, AWRR and TGR. These transitional zones are not all suffering from widespread groundwater stress. For example, climate variables explain 90% of the irrigation variability for summer crops in the MR while groundwater decline is relatively small (0.6 cm/yr) as compared to that for the CR (3 cm/yr) and the AWRR (2.1 cm/yr). This geographical disconnects between regions of climate sensitive irrigation and regions of current water stress is even more clear for humid regions. For instance, spring-autumn crops in the relatively cool, humid PNR are highly sensitive to both precipitation and temperature, but under current conditions the average rate of groundwater depletion in this region is small relative to basins in other parts of the country, in large part because surface water supplies buffer against overexploitation of groundwater. Note that although the net change in groundwater storage in the aquifer system for PNR is subtle, local depletion exists in the deeper hydrogeologic unit where surface water imports are limited [*Konikow*, 2013]. This geographical disconnect is relevant when assessing sustainability of groundwater resources under climate change, though the lack of a large-scale groundwater depletion signal today does not mean that there is no risk of local, seasonal, or future groundwater pressures.

Our simulations are performed at a relatively coarse resolution, such that each "irrigated" grid cell contains a mosaic of irrigated and non-irrigated land. Regression results are sensitive to the choice of which grid cells qualify as "irrigated." As shown in Table S2 and S3, the inferred effect of climate variables on irrigation demand shift as the percent irrigated threshold rises. For

instance, for summer crops in LMR, as the threshold is raised from 30% to 50%, variance in irrigation water that can be explained by climate terms increases from 71% to 80%, and the contribution of T and the interaction term increase and become significant while the effect of P becomes marginal. In contrast, for crops in the TGR and the PNR, sensitivity to precipitation increases for higher irrigation fractions. Greater groundwater declines are found in more intensively irrigated grid cells regardless of the locations and growing season types, implying that simulated groundwater changes are dominated by irrigation. This sensitivity to threshold, however, does not affect the overall character of the results.

Overall, simulated irrigation water use is more sensitive to precipitation variability than it is to temperature variability or the interaction between P and T across most of CONUS. Our regressions leave more unexplained variance in basins that include significant internal climate variability, suggesting that major basin delineations do not sufficiently resolve climate sensitivities of irrigation in these regions. Looking at the problem in gridded regression analysis (Figure 6), we observe intra-basin variability as described above (for example, northern versus southern CR). We also observe clusters of significant temperature sensitivity in the Upper Colorado River basin and several other basins that did not stand out in basin-averaged analysis. We also see widespread negative P by T interaction across the Great Plains, including the MRB and other areas that did not appear as significant in basin averaged analysis. As described above, a negative P by T term indicates greater irrigation sensitivity to P deficit under warmer temperatures. This tendency across the Great Plains, including the High Plains Aquifer region, points to a potential for emerging climate sensitivity in a heavily irrigated region.

3.4 Comparison with observations

Evaluation of the realism of model responses is challenging, on account of both the model's limited ability to account for management decisions and the limited availability of data at a temporal scale fine enough to represent interannual variability in growing season water use. Drawing on publicly available databases, we use statewide calendar year water use reports for Texas, Kansas and Mississippi, and simulated water year total demand for California generated by the California Simulation of Evapotranspiration of Applied Water (Cal-SIMETAW) system as the best available datasets to evaluate our model performance. These State reports do not offer a perfect comparison for our model results, as the reports draw on multiple data sources associated with their own uncertainties. They are also qualitatively different from our simulation in that our model is based on a soil moisture deficit approach that does not explicitly consider irrigation efficiency or human management and adaptation strategies, which may be particularly important under drought conditions. Despite the differences in the magnitude of irrigation water amount, correlations between the simulated and reported irrigation amounts are relatively high, indicating that the model can properly capture interannual variability in irrigation amounts. With these caveats in mind, we examine the simulated and reported sensitivity of irrigation applications to P, T and the interaction between P and T in these four states.

For reported water use in Texas and California, the effect of P is significant and negative, while the effect of T is marginal and the interaction term is significant (Figure 7). The model matches these results in sign and statistical significance, but with quantitatively different regression coefficients. Interestingly, the sign of the interaction term differs between Texas and California. In Texas, warmer conditions strengthen the effect of P shortfall on irrigation water use (negative interaction term), while in California warmer conditions reduce the impact of

precipitation deficit (positive interaction). The Texas result is more intuitive, as warmer conditions increase potential evapotranspiration and might be expected to increase the need to irrigate under precipitation deficit. The California result is possibly led by active management or crop failure in response to dry and hot conditions. As GVF in the intensely irrigated Central Valley is observed to drop under warmer conditions, it is possible that the interaction term captures the fact that crops are less extensive in hot years, resulting in lower sensitivity of total irrigation water to precipitation. This interpretation, however, requires further research. For both the model and observation-derived estimates, irrigation water use in Mississippi is not a strong function of short-term climate; none of the three terms are significant predictors of interannual variability. This could indicate that for this humid environment, atmospheric variations are not dominate factors affecting human management such as prescribing limitations on water use in dry and hot years as the water supply may still be relatively sufficient under these conditions. Model and observation-based estimates do show the same sign of sensitivity for all three terms, though none are statistically significant.

We also note that the interaction term is smaller in the model than in observations for both Texas and California, further suggesting that management decisions not included in our modeling system have some influence on the interaction between P and T. For Kansas, both P and T have significant impacts on reported irrigation water use, with lower T and P associated with higher irrigation water amount. The interaction term has less effect. However, in the model, the explanatory power of T is much lower, and the coefficient even has the opposite sign compared to the regression for the reported estimates. The variability that is explained by the three terms is also substantially lower in the model (55%) than for reported data (73%).

The net result of these data comparisons is not entirely conclusive. We see that model results and reported estimates are similar in terms of the relative contribution from P and the interaction term. We also see discrepancies between model and reported estimates for the impact of T. These discrepancies could be due to limitations in the model, uncertainties in the reported water use estimates, and noise from off-season data. For example, unlike the analyses performed on the sub-basin scale, that only focused on the effective growing seasons, our comparisons with reported data at state level are performed at annual time scale due to limitations in reported data. To examine whether climate variability that comes from seasons may affect the results, we also report the comparisons that the regression analyses are performed on growing season P and T (Figure S8). The variability of annual P or T may not represent the variability of within-season P or T, especially if the rainy seasons do not overlap the growing seasons, such as in much of California. Results for Kansas is very sensitive to the choice of T, as the reported irrigation amount is fairly insensitive to the growing season temperature. Results for Mississippi indicate that the irrigation variability is more associated with growing season P instead of the annual mean. As we do not have sub-annual data in these reports, however, and as in-season irrigation can be influenced by pre-season P and T via their impact on soil moisture, these seasonally-matched analyses have their own limitations. In none of the cases does the sign of a statistically significant relationship change between Figure 7 and Figure S8.

In presenting these state level case studies, we note that Texas, California and Kansas are not necessarily “typical” in irrigation norms or climate sensitivity. As shown in Table 1, negative simulated irrigation water responses to T are only found for sub-basins within these three states. In all other sub-basins, an increase in T is associated with more irrigation water use. Notably, the decision of whether to perform regression on calendar year or water year can be critical for

regions that rely on snow water sources. To demonstrate this, we evaluate sensitivity of the regression results to the choice of calendar year or water year for the top ten irrigated states (Table S4). The explained variance for California and Arizona increases by 13% and 44%, respectively, when water year averages are used, because snowpack and snowmelt from the Sierra Nevada is the primary source of water supply in California (California Water Plan Update 2018) and snowmelt-driven flows in the Colorado River serve as a major surface water supply for Arizona [Lahmers and Eden, 2018].

From the perspective of understanding climate sensitivity, then these comparisons reinforce our understanding that the simulation results must be interpreted as a partially idealized representation of short-term climate influence on irrigation water use. Our model uses a simple demand-driven irrigation algorithm, which is an obvious idealization. The fact that the model is applied using satellite-derived input (vegetation fraction, land cover, irrigated areas) does account for some influence of management decisions on irrigation water use, in that the area actively irrigated and vegetation status are informed by data, but any decisions beyond those basics are not included at all. The comparisons with reported data provide some sense of how realistically the model performs with respect to short-term climate sensitivity—allowing for the caveats associated with the reported irrigation estimates—but simulated irrigation applications and actual irrigation applications are inherently different and must be understood as such. While the reported irrigation water use is a result of mixed impacts of both natural and human factors, the results demonstrate that its connections with temperature either as an independent term or interacting with precipitation are somewhat significant but may be underrepresented in the model. Although the temperature impact might be indirect, making it difficult to represent explicitly in the model, it is worth further exploration because this may become a large source of uncertainty in estimating the water demand under future warming scenarios. Further studies are needed to investigate the extent to which the human decisions and the relationships between precipitation and irrigation water use are sensitive to temperature.

4. Discussion and Conclusions

Conceptually, the link between precipitation and irrigation is straight-forward: when rain supplies more of the water that a crop requires, irrigation applications can be reduced. The link between temperature and irrigation is more nuanced. High growing season temperatures can increase evaporative demand, drying the soil and increasing the need for irrigation applications. But in some regions, temperature can impose a constraint on the growing season, potentially altering cropping and management patterns in a manner that can be captured by our satellite-informed, demand-driven irrigation model. Temperature and precipitation also interact, as the sensitivity of irrigation to precipitation might increase at higher temperatures that bring greater evaporative demand, but if high temperatures lead to reduced crop area then the sign of the interaction can flip.

It is important to emphasize that our results come from a demand-driven simulation of irrigation water applications. This can be thought of as perfectly rational management—our model does not optimize water use efficiency (it is a representation of standard sprinkler irrigation practices), but it does assume that farmers apply water when it is needed rather than as it is convenient. Under real-world conditions, farmers' incentives to plan their water use may depend on water policy and allocations that vary from farm to farm and state to state. Our use of time-varying GVF in the model can capture some of this by tracking the growing season period

and informing the timing of simulated irrigation applications, but these data have limited resolution in both time and space and might not embody all aspects of irrigation calendar variability across states. Therefore, water demand based on soil moisture deficit may be overly idealized. In particular, it is possible that withdrawals will be overestimated for areas suffering drought, because of the inability to explicitly model the efficiency effects of water conservation decisions and water use restrictions, and underestimated when and where water use is not limited by water availability or water conservation policies, because farmers with unlimited access to water might take a simple irrigation scheduling approach rather than the more efficient demand-informed approach.

Similarly, state and local water conservation policies can impact water use in a manner not easily captured in a generalized demand-driven irrigation model. For example, in 2013 Kansas implemented the 2012 Local Enhanced Management Area (LEMA) program. This program helped the state to surpass its water conservation goals in the first five years (2013-2017), leaving enough water in the aquifer to provide over 1.4 years' worth of historic water needs [Deines et al., 2019]. However, as this water conservation is achieved primarily through improvements in irrigation efficiency and crop choice, rather than reductions in irrigated area, our model is not well suited to capture the impact of the LEMA program. Indeed, our simulation overestimates reported water use in the years 2012-2017 by 84%, though it matched these reports quite well for the period 2002-2010, with a slight overestimation by 5%. In 2014, California established the Sustainable Groundwater Management Act (SGMA), which aims to achieve groundwater sustainability by 2040s. It is not clear whether implementation of this act had any impact within our simulation period, but the overlaying of SGMA policies on California's complex water rights introduces an additional source of uncertainty in model-based estimates of near future water demand.

Beyond these specific conservation and water rights policies, our model has general limitations in its representation of active management. For example, even though our model is able to parameterize irrigation in response to coinciding vegetation conditions through identifying growing season by time-varying GVF, the limitations in temporal and spatial resolution of the datasets and the nonlinear feedback prevent the model from capturing local management actions under drought, which may vary with economic, infrastructure, institutional conditions, as well as the drought's hydrologic characteristics, such as the case of California's 2012-2016 drought [*Lund et al.*, 2018].

Our results are also limited by the fact that the simulations do not incorporate variations in irrigation methods and crop types. For example, the use of a row crop as our standard irrigation target may underestimate the variability of irrigation sensitivities in places like California, where row crops, account for only 8% of the irrigated crops and are well mixed with fruits, vegetables and forage, all of which have different water demands and length of growing period [Lobell et al., 2007]. In addition, for this state, sprinkler irrigation only occupies 18% of irrigated land whereas flood and drip irrigation are more common [*Dieter*, 2018]. In this context, our simulated climate sensitivities must be interpreted as indicative estimates for conventional row crops, and not comprehensive estimates for all cropping systems. Additionally, limitations in the irrigation-related datasets prevent us from exploring climate sensitivity over longer time periods. Temperature sensitivity may be underestimated as the time frame might be too short to capture extreme temperature events and variability at longer temporal scales. Our model's representation of groundwater is also relatively simple. Even in a relatively simple demand-

driven model, however, the influence that climate variability has on irrigation is not always obvious, and the results of modeling exercises can yield insight on regional and seasonal differences in expected climate impacts on irrigation, and hence on water resources. Continued model development is underway to improve the fidelity of the model simulation of local processes, but performance at this level allows us to apply the model at large scale to study general climate sensitivities.

Despite the many assumptions and uncertainties associated with the model, key results of this study include: (1) widespread sensitivity of irrigation water use to precipitation, in both model and available reports (which is logical); (2) regionally and seasonally variable sensitivity to temperature, suggesting differing potential impacts of warming on irrigation water demand; (3) interactions between temperature and precipitation sensitivity that differ by location and might reflect impacts of management decisions and/or crop failure under climate variability; these interaction terms might be underestimated by the model; (4) geographical disconnects between aquifers that are stressed by pumping and the basins that exhibit strong climate sensitivities, which should be considered in assessing future climate impacts and irrigation-based adaptation. For each of these results, management can play a critical role in climate response and resilience strategies.

Acknowledgements

This research is supported in part by the NASA GRACE Science Team award NNX16AF12G. Computational resources were provided by the NASA Center for Climate Simulation (NCCS) at NASA's Goddard Space Flight Center and the Maryland Advanced Research Computing Center (MARCC). Different data sets used for comparison were obtained from various sources described in Methods. The model output is available through Johns Hopkins University Data Archive (https://doi.org/10.7281/T1/AZE8LU). We thank Long Zhao for helpful guidance on the statistical techniques.

References

Asoka, A., T. Gleeson, Y. Wada, and V. Mishra (2017), Relative contribution of monsoon precipitation and pumping to changes in groundwater storage in India, *Nature Geosci*, *10*(2), 109–117.

Baker, J. M., T. J. Griffis, and T. E. Ochsner (2012), Coupling landscape water storage and supplemental irrigation to increase productivity and improve environmental stewardship in the U.S. Midwest, *Water Resour. Res.*, *48*(5), 247, doi:10.1029/2011WR011780.

Brown, J. F., and M. S. Pervez (2014), Merging remote sensing data and national agricultural statistics to model change in irrigated agriculture, *Agricultural Systems*, *127*, 28–40.

Condon, L. E., A. L. Atchley, and R. M. Maxwell (2020), Evapotranspiration depletes groundwater under warming over the contiguous United States, *Nature Communications*, *11*(1), 1–8.

Condon, L. E., & Maxwell, R. M. (2019). Simulating the sensitivity of evapotranspiration and streamflow to large-scale groundwater depletion. Science Advances, 5(6), eaav4574.

de Graaf, I. E. M., T. Gleeson, L. P. H. R. van Beek, E. H. Sutanudjaja, and M. F. P. Bierkens (2019), Environmental flow limits to global groundwater pumping, *Nature*, *574*(7776), 90–94, doi:10.1038/s41586-019-1594-4.

Deines, J. M., A. D. Kendall, J. J. Butler, and D. W. Hyndman (2019), Quantifying irrigation adaptation strategies in response to stakeholder-driven groundwater management in the US High Plains Aquifer, *Environ. Res. Lett.*

Devanand, A., M. Huang, M. Ashfaq, B. Barik, and S. Ghosh (2019), Choice of irrigation water management practice affects indian summer monsoon rainfall and its extremes, *Geophys. Res. Lett.*, *46*(15), 9126–9135.

Dieter, C. (2018), Estimated Use of Water in the United States in 2015, 1–76, doi:https://doi.org/10.3133/cir1441.

Döll, P., H. Hoffmann-Dobrev, F. T. Portmann, S. Siebert, A. Eicker, M. Rodell, G. Strassberg, and B. R. Scanlon (2012), Impact of water withdrawals from groundwater and surface water on continental water storage variations, *Journal of Geodynamics*, *59*, 143–156.

Eicker, A., M. Schumacher, J. Kusche, P. Döll, and H. M. Schmied (2014), Calibration/data assimilation approach for integrating GRACE data into the WaterGAP Global Hydrology Model (WGHM) using an ensemble Kalman filter: First results, *Surveys in Geophysics*, *35*(6), 1285–1309.

Ek, M. B., K. E. Mitchell, Y. Lin, E. Rogers, P. Grunmann, V. Koren, G. Gayno, and J. D. Tarpley (2003), Implementation of Noah land surface model advances in the National Centers for Environmental Prediction operational mesoscale Eta model, *J. Geophys. Res.*, *108*(D22).

670 Evans, J. P., and B. F. Zaitchik (2008), Modeling the large-scale water balance impact of
671 different irrigation systems, *Water Resour. Res.*, *44*(8).

672 Farr, T. G., P. A. Rosen, E. Caro, R. Crippen, R. Duren, S. Hensley, M. Kobrick, M. Paller, E.
673 Rodriguez, and L. Roth (2007), The shuttle radar topography mission, *Reviews of*
674 *geophysics*, *45*(2).

675 Felfelani, F., Y. Pokhrel, K. Guan, and D. M. Lawrence (2018), Utilizing SMAP soil moisture
676 data to constrain irrigation in the Community Land Model, *Geophys. Res. Lett.*, *45*(23), 12–
677 892–12–902.

678 Gurdak, J. J. (2017), Groundwater: Climate-induced pumping, *Nature Geosci*, *10*(2), 71–71.

679 Jasechko, S., Perrone, D., Befus, K. M., Cardenas, M. B., Ferguson, G., Gleeson, T., ... &
680 Kirchner, J. W. (2017). Global aquifers dominated by fossil groundwaters but wells
681 vulnerable to modern contamination. *Nature Geoscience, 10*(6), 425-429.

682 Konikow, L. F. (2013). Groundwater depletion in the United States (1900-2008). Reston,
683 Virginia: US Department of the Interior, US Geological Survey.

684 Kumar, S. V., C. D. Peters-Lidard, Y. Tian, P. R. Houser, J. Geiger, S. Olden, L. Lighty, J. L.
685 Eastman, B. Doty, and P. Dirmeyer (2006), Land information system: An interoperable
686 framework for high resolution land surface modeling, *Environmental modelling & software*,
687 *21*(10), 1402–1415.

688 Lahmers, T., and S. Eden (2018), Water and Irrigated Agriculture in Arizona, *Arroyo. University*
689 *of Arizona Water Resources Research Center, Tucson, AZ.*

690 Lawston, P. M., J. A. Santanello Jr, and S. V. Kumar (2017), Irrigation signals detected from
691 SMAP soil moisture retrievals, *Geophys. Res. Lett.*, *44*(23), 11–860–11–867.

692 Lawston, P. M., J. A. Santanello Jr, B. F. Zaitchik, and M. Rodell (2015), Impact of irrigation
693 methods on land surface model spinup and initialization of WRF forecasts, *J. Hydrometeor.*,
694 *16*(3), 1135–1154.

695 Leng, G., M. Huang, Q. Tang, H. Gao, and L. R. Leung (2014), Modeling the effects of
696 groundwater-fed irrigation on terrestrial hydrology over the conterminous United States, *J.*
697 *Hydrometeor.*, *15*(3), 957–972.

698 Leng, G., M. Huang, Q. Tang, W. J. Sacks, H. Lei, and L. R. Leung (2013), Modeling the effects
699 of irrigation on land surface fluxes and states over the conterminous United States:
700 Sensitivity to input data and model parameters, *J. Geophys. Res. Atmos.*, *118*(17), 9789–
701 9803.

702 Liu, Z., Liu, P. W., Massoud, E., Farr, T. G., Lundgren, P., & Famiglietti, J. S. (2019).
703 Monitoring Groundwater Change in California's Central Valley Using Sentinel-1 and
704 GRACE Observations. Geosciences, 9(10), 436.

Lobell, D. B., K. N. Cahill, and C. B. Field (2007), Historical effects of temperature and precipitation on California crop yields, *Climatic change*, *81*(2), 187–203.

Lund, J., J. Medellin-Azuara, J. Durand, and K. Stone (2018), Lessons from California's 2012–2016 Drought, *J. Water Resour. Plann. Manage.*, *144*(10), 04018067–13, doi:10.1061/(ASCE)WR.1943-5452.0000984.

Massey, J. H., C. M. Stiles, J. W. Epting, R. S. Powers, D. B. Kelly, T. H. Bowling, C. L. Janes, and D. A. Pennington (2017), Long-term measurements of agronomic crop irrigation made in the Mississippi delta portion of the lower Mississippi River Valley, *Irrigation Science*, *35*(4), 297–313, doi:10.1007/s00271-017-0543-y.

McDermid, S. S., L. O. Mearns, and A. C. Ruane (2017), Representing agriculture in E arth S ystem M odels: Approaches and priorities for development, *J. Adv. Model. Earth Syst.*, *9*(5), 2230–2265.

Nazemi, A., and H. S. Wheater (2015), On inclusion of water resource management in Earth system models--Part 2: Representation of water supply and allocation and opportunities for improved modeling, *Hydrol. Earth Syst. Sci.*, *19*(1).

Nie, W., B. F. Zaitchik, M. Rodell, S. V. Kumar, K. R. Arsenault, B. Li, and A. Getirana (2019), Assimilating GRACE into a Land Surface Model in the presence of an irrigation-induced groundwater trend, *Water Resour. Res.*

Nie, W., B. F. Zaitchik, M. Rodell, S. V. Kumar, M. C. Anderson, and C. Hain (2018), Groundwater withdrawals under drought: Reconciling GRACE and land surface models in the United States High Plains Aquifer, *Water Resour. Res.*, *54*(8), 5282–5299.

Niu, G. Y., Yang, Z. L., Mitchell, K. E., Chen, F., Ek, M. B., Barlage, M., ... & Tewari, M. (2011). The community Noah land surface model with multiparameterization options (Noah-MP): 1. Model description and evaluation with local-scale measurements. Journal of Geophysical Research: Atmospheres, 116(D12).

Niu, G. Y., Z. L. Yang, R. E. Dickinson, L. E. Gulden, and H. Su (2007), Development of a simple groundwater model for use in climate models and evaluation with Gravity Recovery and Climate Experiment data, *J. Geophys. Res.*, *112*(D7).

Orang, M. N., R. L. Snyder, G. Shu, Q. J. Hart, S. Sarreshteh, M. Falk, D. Beaudette, S. Hayes, and S. Eching (2013), California simulation of evapotranspiration of applied water and agricultural energy use in California, *Journal of Integrative Agriculture*, *12*(8), 1371–1388.

Ozdogan, M., M. Rodell, H. K. Beaudoing, and D. L. Toll (2010), Simulating the effects of irrigation over the United States in a land surface model based on satellite-derived agricultural data, *Journal of Hydrometeorology*, *11*(1), 171–184.

Pokhrel, Y. N., N. Hanasaki, Y. Wada, and H. Kim (2016), Recent progresses in incorporating human land–water management into global land surface models toward their integration into Earth system models, *Wiley Interdisciplinary Reviews: Water*, *3*(4), 548–574.

742 Pokhrel, Y. N., S. Koirala, P. J.-F. Yeh, N. Hanasaki, L. Longuevergne, S. Kanae, and T. Oki
743 (2015), Incorporation of groundwater pumping in a global L and S urface M odel with the
744 representation of human impacts, *Water Resour. Res.*, *51*(1), 78–96.

745 Pokhrel, Y., N. Hanasaki, S. Koirala, J. Cho, P. J.-F. Yeh, H. Kim, S. Kanae, and T. Oki (2012),
746 Incorporating anthropogenic water regulation modules into a land surface model, *J.*
747 *Hydrometeor.*, *13*(1), 255–269.

748 Rodell, M., J. S. Famiglietti, D. N. Wiese, J. T. Reager, H. K. Beaudoing, F. W. Landerer, and
749 M.-H. Lo (2018), Emerging trends in global freshwater availability, *Nature*, *557*(7707), 651–
750 659.

751 Russo, T. A., and U. Lall (2017), Depletion and response of deep groundwater to climate-
752 induced pumping variability, *Nature Geosci*, *10*(2), 105–108.

753 Scanlon, B. R., C. C. Faunt, L. Longuevergne, R. C. Reedy, W. M. Alley, V. L. McGuire, and P.
754 B. McMahon (2012), Groundwater depletion and sustainability of irrigation in the US High
755 Plains and Central Valley, *Proc Natl Acad Sci USA*, *109*(24), 9320–9325.

756 Scanlon, B. R., Z. Zhang, H. Save, A. Y. Sun, H. M. Schmied, L. P. Van Beek, D. N. Wiese, Y.
757 Wada, D. Long, and R. C. Reedy (2018), Global models underestimate large decadal
758 declining and rising water storage trends relative to GRACE satellite data, *Proc Natl Acad*
759 *Sci USA*, *115*(6), E1080–E1089.

760 Schewe, J., J. Heinke, D. Gerten, I. Haddeland, N. W. Arnell, D. B. Clark, R. Dankers, S. Eisner,
761 B. M. Fekete, and F. J. Colón-González (2014), Multimodel assessment of water scarcity
762 under climate change, *Proc Natl Acad Sci USA*, *111*(9), 3245–3250.

763 Schwarz, G. E., and R. B. Alexander (1995), State soil geographic (STATSGO) data base for the
764 conterminous United States (No. 95-449).

765 Siebert, S., J. Burke, J.-M. Faures, K. Frenken, J. Hoogeveen, P. Döll, and F. T. Portmann
766 (2010), Groundwater use for irrigation—a global inventory, *Hydrol. Earth Syst. Sci.*, *14*(10),
767 1863–1880.

768 Valley, S. (2009), Groundwater availability of the Central Valley aquifer, California, *US*
769 *Geological Survey professional paper*.

770 Van Beek, L., Y. Wada, and M. F. Bierkens (2011), Global monthly water stress: 1. Water
771 balance and water availability, *Water Resour. Res.*, *47*(7).

772 Wada, Y., D. Wisser, and M. F. P. Bierkens (2014), Global modeling of withdrawal, allocation
773 and consumptive use of surface water and groundwater resources, *Earth Syst. Dynam.*, *5*(1),
774 15–40, doi:10.5194/esd-5-15-2014.

775 Wada, Y., L. P. Van Beek, C. M. Van Kempen, J. W. Reckman, S. Vasak, and M. F. Bierkens
776 (2010), Global depletion of groundwater resources, *Geophys. Res. Lett.*, *37*(20).

Wada, Y., M. F. Bierkens, A. De Roo, P. A. Dirmeyer, J. S. Famiglietti, N. Hanasaki, M. Konar, J. Liu, H. M. Schmied, and T. Oki (2017), Human-water interface in hydrological modelling: current status and future directions, *Hydrol. Earth Syst. Sci.*, *21*(8), 4169–4193.

Wiese, D. N., F. W. Landerer, and M. M. Watkins (2016), Quantifying and reducing leakage errors in the JPL RL05M GRACE mascon solution, *Water Resour. Res.*, *52*(9), 7490–7502.

Xia, Y., K. Mitchell, M. Ek, J. Sheffield, B. Cosgrove, E. Wood, L. Luo, C. Alonge, H. Wei, and J. Meng (2012), Continental-scale water and energy flux analysis and validation for the North American Land Data Assimilation System project phase 2 (NLDAS-2): 1. Intercomparison and application of model products, *J. Geophys. Res. Atmos.*, *117*(D3).

Yang, Z. L., G. Y. Niu, K. E. Mitchell, F. Chen, M. B. Ek, M. Barlage, L. Longuevergne, K. Manning, D. Niyogi, and M. Tewari (2011), The community Noah land surface model with multiparameterization options (Noah-MP): 2. Evaluation over global river basins, *J. Geophys. Res.*, *116*(D12).

Yilmaz, M. T., M. C. Anderson, B. Zaitchik, C. R. Hain, W. T. Crow, M. Ozdogan, J. A. Chun, and J. Evans (2014), Comparison of prognostic and diagnostic surface flux modeling approaches over the Nile River basin, *Water Resour. Res.*, *50*(1), 386–408.

Yin, Z., X. H. Wang, C. Ottlé, F. Zhou, M. Guimberteau, J. Polcher, S. S. Peng, S. L. Piao, L. Li, and Y. Bo (2020), Improvement of the irrigation scheme in the ORCHIDEE land surface model and impacts of irrigation on regional water budgets over China, *J. Adv. Model. Earth Syst.*, *12*(4), e2019MS001770.

Zou, Z., Xiao, X., Dong, J., Qin, Y., Doughty, R. B., Menarguez, M. A., ... & Wang, J. (2018). Divergent trends of open-surface water body area in the contiguous United States from 1984 to 2016. Proceedings of the National Academy of Sciences, 115(15), 3810-3815.

Figure 1. The (a) irrigation fraction from the MODIS Irrigated Agriculture Dataset for the United States (MIrAD-US) for 2002, and (b) percent of irrigation from groundwater derived from the USGS water use report for 2000 over CONUS. Color highlighted areas are Pacific Northwest (PNR), California (CR), Missouri (MR), Arkansas-White-Red (AWRR), Texas-Gulf (TGR), Upper Mississippi (UMR), Lower Mississippi (LMR), Great Lakes (GLR), and South Atlantic-Gulf (SAGR) water resource regions.

Figure 2. The (a) irrigation fraction (extracted from MIrAD-US), using 2002 as reference, and (b) percent of irrigation from groundwater (extracted from the USGS water use report) for the reference year of 2000. The differences between the reference years and the other available years at 5-year intervals for the nine water resources regions, respectively.

Figure 3. (a) Comparison of the observed and simulated groundwater (GW) and surface water (SW) irrigation amount for the top 10 irrigated states, selected and ranked based on averaged total irrigation amount for 2005, 2010 and 2015; (b) scatter plot of simulated total against

observed consumptive irrigation amount for 2015, with the colors and sizes of the triangles indicating annual precipitation level (P) and temperature level (T), respectively.

Figure 4. The (a) distribution of correlation coefficients for simulated irrigation water use against NLDAS2-based precipitation (P) and temperature (T) for active irrigated grid cells and (b) percent of the active irrigated area that has statistically significant correlation values at the 5% level for nine major growing season types. The correlation is calculated based on annual averaged values during the growing seasons.

Figure 5. Averaged seasonal cycle of (a) precipitation and (b) temperature (drawn from NLDAS2 forcing datasets) in active irrigated area for nine major irrigated river basins, 2002-2017.

Figure 6. The sensitivity of simulated irrigation water use to climate variability (P, T and the interactive term PT, all drawn from NLDAS-2 forcing data) for actively irrigated areas. The regression analysis is performed at grid cell scale and the sign indicates either positive or negative contribution, with the circle sizes varying among P (large), T (medium) and PT (small). Grid cells with insignificant regression coefficients (at the 95% confidence level) or fail to pass the Shapiro-Wilk test are masked as "insensitive" (dark grey circles). Water resource regions are ranked in terms of groundwater decline (darker gray indicating a greater decline) over actively irrigated areas within each region.

Figure 7. Comparison between the simulated and reported statewide annual total irrigation amount for (a) Texas, (b) California, (c) Kansas and (d) Mississippi. Bar plot denotes the regression coefficient for P, T and their interaction term, with the star indicating the significance at 95% confidence level. Black circle indicates R-Squared values. Blue diamond denotes the correlation between the simulated and reported annual irrigation time series with the filled diamonds indicating the significance at the 95% confidence level.

Table 1. Summary statistics for regressions that predict modeled irrigation water use as a function of climate variables (P, T, and the P by T interactive term), along with groundwater storage trends for each study region. Results are shown for major growing season types in each region. Colors are similar to Figure 6, but with different saturation levels used to show the magnitude of coefficients: blue for precipitation coefficients, red (yellow) for positive (negative) temperature coefficients, and green (brown) for positive (negative) interaction term.

	PNR			CR		MR	AWRR		TGR				UMR	LMR	GLR	SAGR
	Su	Sp	Sp–Au	Sp	Su	Su	Su	Au	Sp	Au	Su	Sp–Au	Su	Su	Su	Su
β_T	0.01	0.26**	0.52*	0.19	−0.36	0.20**	0.22	−0.20	0.20	0.21	−0.07	0.24	0.27	0.20	0.59*	0.02
β_P	−0.85*	−0.73*	−0.73*	−0.44	−0.48**	−0.75*	−0.56*	−1.30*	−0.65**	−0.70*	−0.91*	−0.62*	−0.35	−0.65*	−0.30	−0.65
$\beta_{P\&T}$	−0.05	0.00	0.04	0.19	0.32	−0.05	−0.09	−0.74*	−0.10	−0.35**	−0.19*	−0.15	−0.48	0.16	−0.20	0.05
R^2	0.71	0.8	0.68	0.41	0.33	0.9	0.72	0.81	0.58	0.67	0.9	0.68	0.74	0.62	0.4	0.5
GW_{TR}(cm/yr)	−0.8*	−1.*	−0.3*	−1.*	−3.*	−0.6*	−2.1*	−3.8*	−0.4*	−1.4*	−2.3*	−2.*	−0.1	−0.1	0.	0.

* and ** represent coefficients that are statistically significant at the 95% and 90% confidence level respectively.

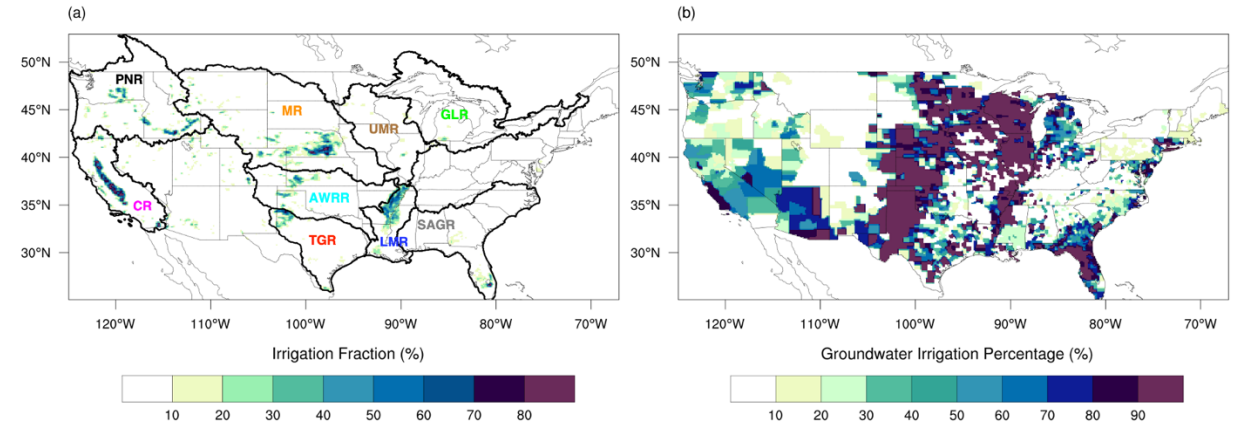

849

850 **Figure 1.** The (a) irrigation fraction from the MODIS Irrigated Agriculture Dataset for the
851 United States (MIrAD-US) for 2002, and (b) percent of irrigation from groundwater derived
852 from the USGS water use report for 2000 over CONUS. Color highlighted areas are Pacific
853 Northwest (PNR), California (CR), Missouri (MR), Arkansas-White-Red (AWRR), Texas-Gulf
854 (TGR), Upper Mississippi (UMR), Lower Mississippi (LMR), Great Lakes (GLR), and South
855 Atlantic-Gulf (SAGR) water resource regions.

856

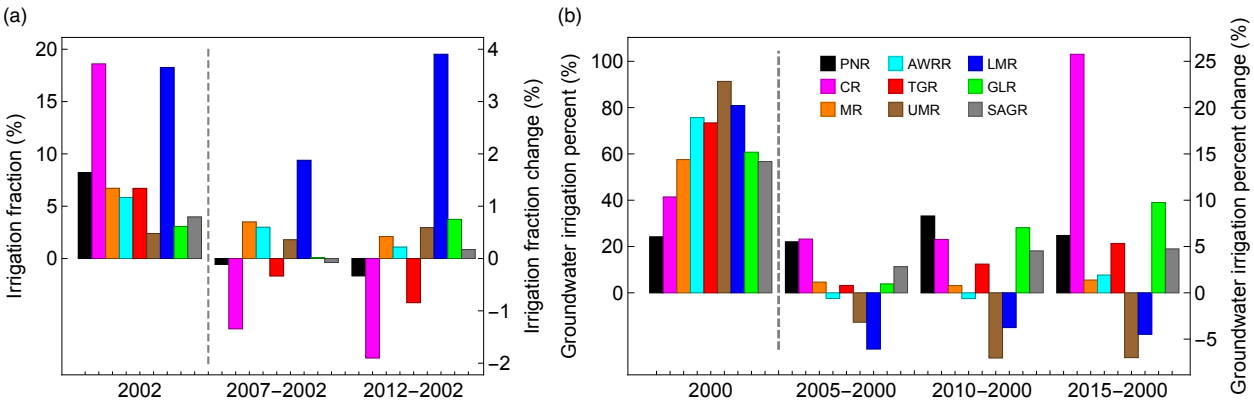

857

858 **Figure 2.** The (a) irrigation fraction (extracted from MIrAD-US), using 2002 as reference, and
859 (b) percent of irrigation from groundwater (extracted from the USGS water use report) for the
860 reference year of 2000. The differences between the reference years and the other available years
861 at 5-year intervals for the nine water resources regions, respectively.
862

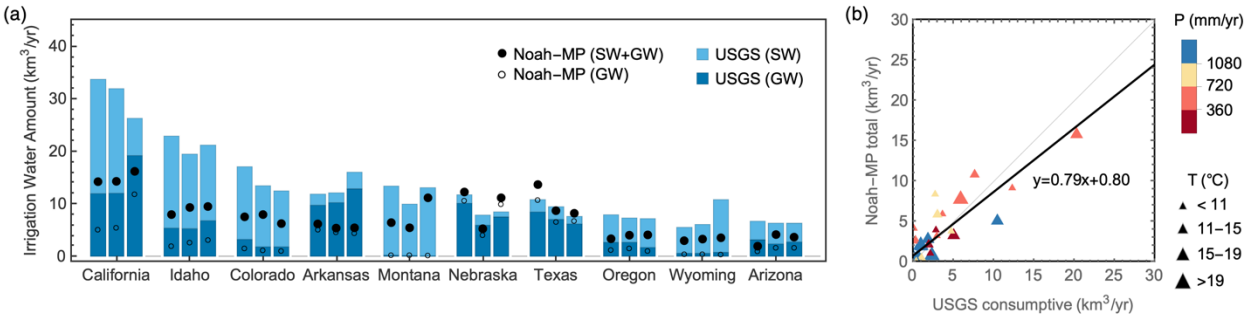

863

864 **Figure 3.** (a) Comparison of the observed and simulated groundwater (GW) and surface water
865 (SW) irrigation amount for the top 10 irrigated states, selected and ranked based on averaged
866 total irrigation amount for 2005, 2010 and 2015; (b) scatter plot of simulated total against
867 observed consumptive irrigation amount for 2015, with the colors and sizes of the triangles
868 indicating annual precipitation level (P) and temperature level (T), respectively.

869

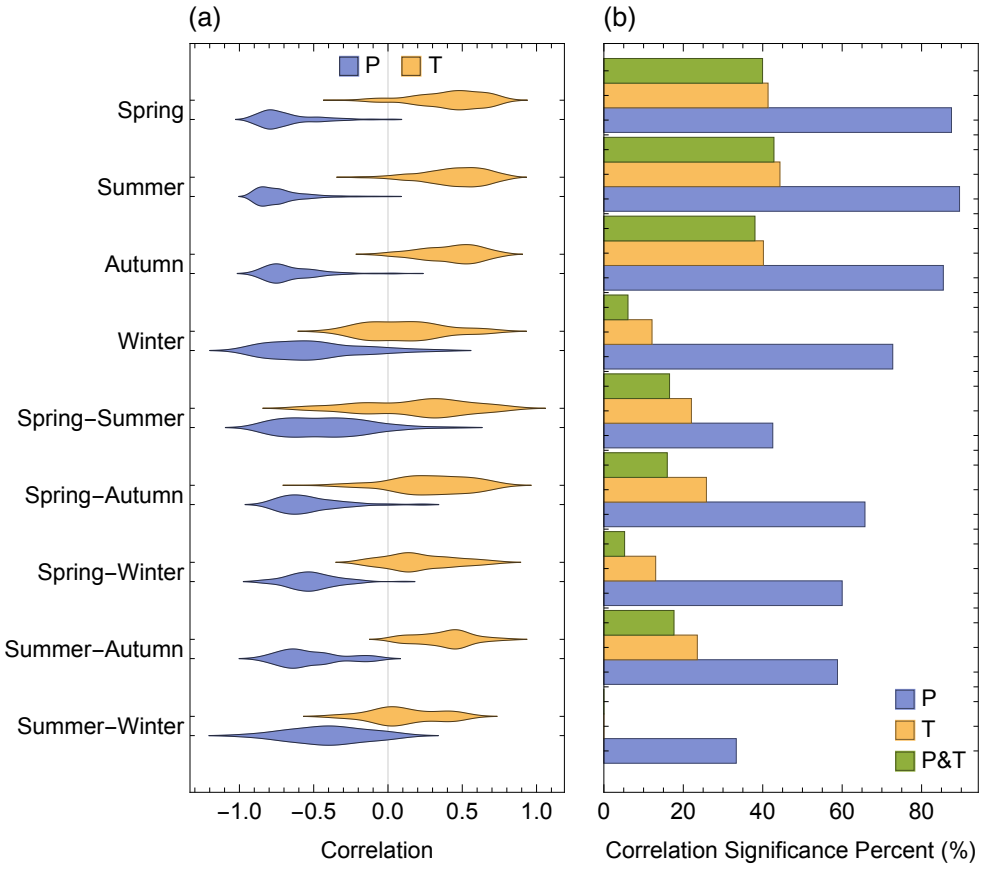

870

871 **Figure 4.** The (a) distribution of correlation coefficients for simulated irrigation water use
872 against NLDAS2-based precipitation (P) and temperature (T) for active irrigated grid cells and
873 (b) percent of the active irrigated area that has statistically significant correlation values at the
874 5% level for nine major growing season types. The correlation is calculated based on annual
875 averaged values during the growing seasons.

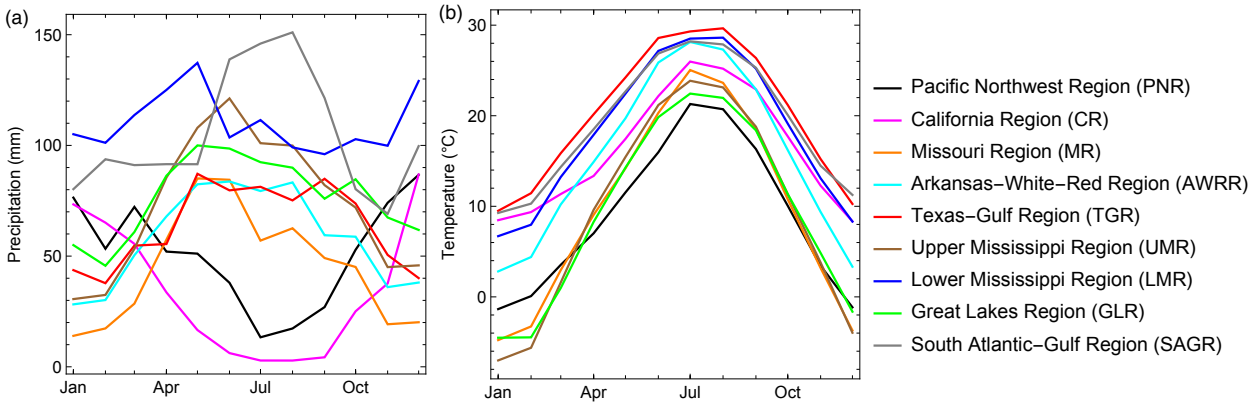

Figure 5. Averaged seasonal cycle of (a) precipitation and (b) temperature (drawn from NLDAS2 forcing datasets) in active irrigated area for nine major irrigated river basins, 2002-2017.

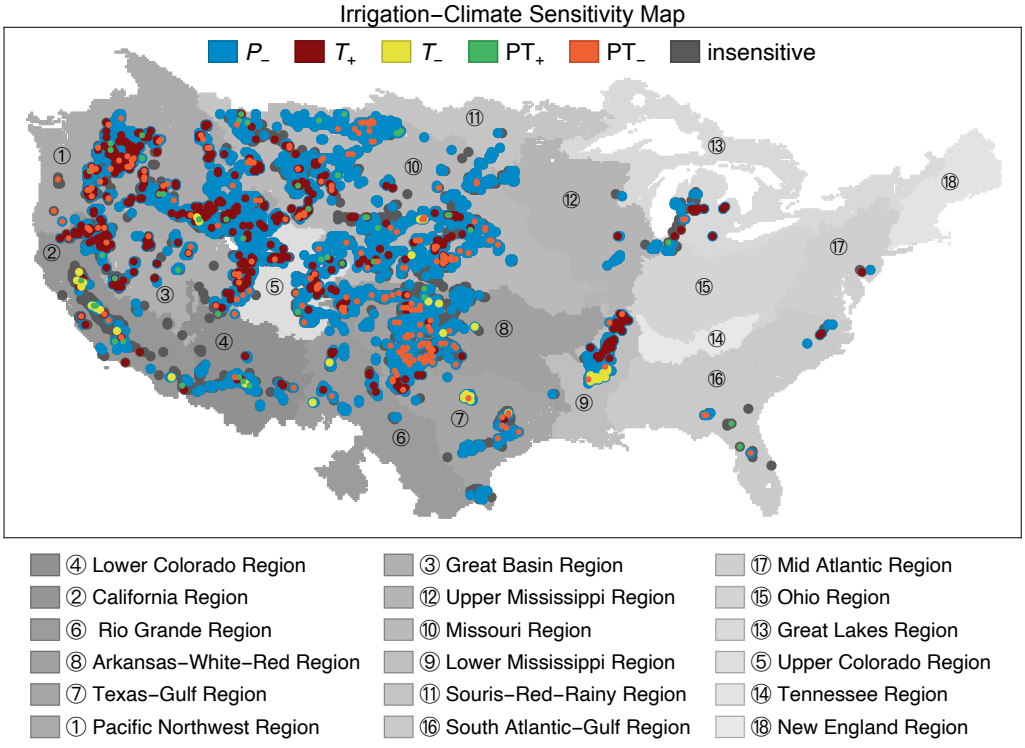

Figure 6. The sensitivity of simulated irrigation water use to climate variability (P, T and the interactive term PT, all drawn from NLDAS-2 forcing data) for actively irrigated areas. The regression analysis is performed at grid cell scale and the sign indicates either positive or negative contribution, with the circle sizes varying among P (large), T (medium) and PT (small). Grid cells with insignificant regression coefficients (at the 95% confidence level) or fail to pass the Shapiro-Wilk test are masked as "insensitive" (dark grey circles). Water resource regions are ranked in terms of groundwater decline (darker gray indicating a greater decline) over actively irrigated areas within each region.

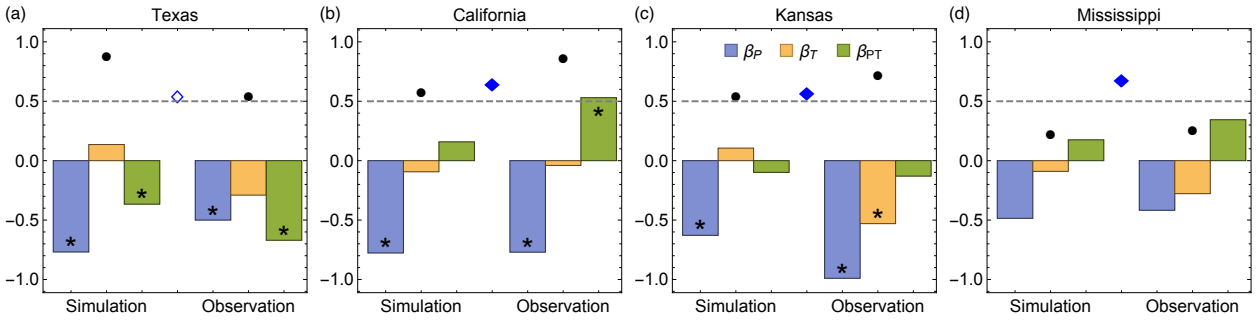

Figure 7. Comparison between the simulated and reported statewide annual total irrigation amount for (a) Texas, (b) California, (c) Kansas and (d) Mississippi. Bar plot denotes the regression coefficient for P, T and their interaction term, with the star indicating the significance at 95% confidence level. Black circle indicates R-Squared values. Blue diamond denotes the correlation between the simulated and reported annual irrigation time series with the filled diamonds indicating the significance at the 95% confidence level.